Araştırma Makalesi *BAUN Fen Bil. Enst. Dergisi, 26(2), 455-471, (2024)*

DOI:10.25092/baunfbed. 1297146 *J. BAUN Inst. Sci. Technol., 26(2), 455-471, (2024)*

Activated carbon assisted cobalt catalyst for hydrogen production: synthesis and characterization

Selma EKİNCİ[1,*], Erhan ONAT[2]

[1,*] *Batman University, Vocational School of Technical Sciences, Department of Chemistry and Chemical Process Technology, Batman, Turkey.*
[2] *Bitlis Eren University, Vocational School of Organized Industrial Zone, Department of Electrical and Energy, Bitlis, Turkey.*

Geliş Tarihi (Received Date): 15.05.2023
Kabul Tarihi (Accepted Date): 01.05.2024

Abstract

In this work, a cobalt catalyst supported by activated carbon was used to produce hydrogen through the hydrolysis of sodium borohydride ($NaBH_4$). First, hydrochar was produced from MDF powder by hydrothermal pretreatment. Then, ideal parameters (activator percentage, activation time, baking time, and temperature) for activated carbon production were determined. The best conditions for the synthesis of activated carbon were found to be a 70% activator rate, 24 hours of activation time, 45 minutes of baking time, and 700 ºC temperature, according to iodine number measurements. The iodine number was measured as 929 mg/g under optimum conditions. Activated carbon (as a support) produced under optimum conditions was combined with the cobalt catalyst. DT/TGA, FT-IR, SEM, and EDX analyses were used to evaluate the catalyst's structure. Supporting material ratio, NaOH concentration, catalyst amount, and $NaBH_4$ concentration are the variables studied in catalyst synthesis. The trials led to the identification of the optimal catalyst parameters as being 70% support material, 5% NaOH, 40 mg catalyst, and 2% $NaBH_4$ concentration. The hydrogen production rate with the catalyst synthesized in these conditions was determined as 8592.8 ml/g.min. As a result of the hydrolysis reactions carried out at different temperatures, it was determined that the reaction was n. order and the reaction activation energy was 31.19 kJ/mol. Even after the sixth use, 100% efficiency was attained when the catalyst activity was tested repeatedly.

Keywords: *Co@AC catalyst, supported catalyst, hydrogen, sodium borohydride*

---

[*] Selma EKİNCİ, selma.ekinci@batman.edu.tr, https://orcid.org/0000-0002-7835-4832
Erhan ONAT, eonat@beu.edu.tr, https://orcid.org/0000-0003-1638-0151

Hidrojen üretimi için aktif karbon destekli kobalt katalizörü: sentez ve karakterizasyon

Öz

Bu çalışmada, sodyum borhidrürün ($NaBH_4$*) hidrolizi yoluyla hidrojen üretmek için aktif karbonla desteklenen bir kobalt katalizörü kullanıldı. İlk olarak, hidrotermal ön işlem ile MDF tozundan hidrokömür üretildi. Daha sonra, aktif karbon üretimi için ideal parametreler (aktifleştirici yüzdesi, aktivasyon süresi, fırınlanma süresi ve sıcaklık) belirlendi. Aktif karbon sentezi için en iyi koşullar iyot sayısı ölçümlerine göre %70 aktifleştirici oranı, 24 saat aktivasyon süresi, 45 dakika fırınlanma süresi ve 700 ⁰C sıcaklık olarak belirlendi. İyot sayısı optimum koşullarda 929 mg/g olarak ölçüldü. Kobalt katalizörü ile optimum koşullarda üretilmiş aktif karbon (destek maddesi) birleştirildi. Katalizörün yapısını değerlendirmek için DT/TGA, FT-IR, SEM ve EDX analizleri kullanıldı. Destekleyici malzeme oranı, NaOH konsantrasyonu, katalizör miktarı ve *$NaBH_4$* konsantrasyonu, katalizör sentezinde incelenen değişkenlerdir. Katalizör sentezi için optimum parametreler, %70 destek malzemesi, %5 NaOH, 40 mg katalizör ve %2 *$NaBH_4$* konsantrasyonu olarak belirlendi. Bu koşullarda sentezlenen katalizör ile hidrojen üretim hızı 8592.8 ml/g.dk olarak hesaplandı. Farklı sıcaklıklarda gerçekleştirilen hidroliz reaksiyonları sonucunda reaksiyonun n. dereceden ve aktivasyon enerjisinin de 31.19 kJ/mol olduğu belirlendi. Altıncı kullanımdan sonra bile katalizör aktivitesi tekrar tekrar test edildiğinde %100 verim elde edildi.*

Anahtar kelimeler: *Co@AC katalizörü, destekli katalizör, hidrojen, sodyum borhidrür*

1. Introduction

Fossil fuels are the main source of energy, which is one of the needs for the continued development of humanity. The limited supply of these fuels and the harm their byproducts cause to the environment have prompted humanity to look for alternate energy sources. One of the topics that scientists are now conducting the most study on is energy sources that could replace fossil fuels. The most intriguing study topic among these alternate sources is hydrogen, which can transport energy [1,2].

The fact that hydrogen may be supplied from a variety of sources is the main justification for using it as a transporter of energy. Water, coal, natural gas, oil, boron hydrides, organic compounds, and inorganic materials make up the majority of these resources [3,4].

Another benefit of using hydrogen as an energy source is that, unlike fossil fuels, its byproducts are environmentally neutral and help reduce the greenhouse gas effect. Hydrogen, which is used in energy production through fuel cells called Proton Exchange Membrane (PEM), releases water vapor to nature as a waste material. Despite being actively used in the creation of energy from hydrogen, PEM fuel technology is still evolving. The issue of transportation and storage is the main barrier to using hydrogen as a direct energy carrier in fuel cells. Since these cells currently use gaseous hydrogen, doing so incurs additional costs and safety risks. The chemical deposition of hydrogen in metal hydride complexes effectively solves this issue [5]. Due to these advantages, boron (B) based metal hydrides ($NaBH_4$, KBH_4, $Ca(BH_4)_2$, $Mg(BH_4)_2$) have been studied intensively since the early 2000s [6,7].

In general, Equation 1 describes the controlled decomposition reaction of metal hydrides produced from boron in the presence of a catalyst [8].

$$MeBH_4 + 2\,H_2O \rightarrow MeBO_2 + 4H_2 \qquad (1)$$

Sodium boron hydride ($NaBH_4$) provides chemical storage of hydrogen. The storage and transportation issues associated with using hydrogen for energy production are mostly resolved by this feature. $NaBH_4$, one of the most used metal hydrides, is also employed in the production of many steroids and vitamin A. It is also used as a reducing agent in the production of gold nanoparticles. However, since it already has hydrogen in its structure, the most crucial application is as a hydrogen storage facility. Theoretically, it contains 10.8% hydrogen in its structure.

$$NaBH_4 + 2H_2O \rightarrow NaBO_2 + 4H_2 \qquad (2)$$

Equation 2 demonstrates how the sodium borohydride hydrolysis reaction makes it possible to extract as much hydrogen from water as is present in its structure. As a result, the issues with hydrogen storage and transportation are solved, and water can also be used to produce some of the flexible hydrogen needed for hydrogen fuel cells. With the help of the catalyst, the rate of the reaction shown in Equation 2 can be controlled [9-10].

Catalysts are substances that speed up a chemical reaction that is thermodynamically voluntary. In most cases, catalysts alter the reaction's activation energy (Ea), enabling it to proceed via a different pathway. Sometimes, a change in the mechanism takes the form of adding or subtracting reaction steps. The key elements that determine the catalyst's efficiency include parameters like the surface area of the catalyst and the activity of the chemicals used [11]. Depending on how it interacts with the substrate it operates on, the catalyst is referred to as either a homogeneous or a heterogeneous catalyst. In general, a catalyst is referred to as homogeneous if it is in the same state as the substrate, and a heterogeneous catalyst if it is in a different state. Heterogeneous catalysts are utilized more frequently in terms of facile recovery and reaction rate control among these catalyst types, which each have advantages and disadvantages. Although catalysts are generally substances that increase the reaction rate, some catalysts decrease the reaction rate. Catalysts that reduce the reaction rate are called inhibitors [12].

An effective catalyst needs to have a great deal of surface area. The materials that give the catalysts more surface area can differ greatly in their characteristics. Support materials are those substances that boost the catalyst's efficiency and surface area [13]. The most popular support materials are graphene oxide, activated carbon, Al_2O_3, and various polymer compounds. These components decrease the cost of the catalyst while also improving its effectiveness. Because, in addition to their high efficiency, the materials used as catalysts are expensive economically. Low-cost support materials are obtained at reasonable prices [14]. Since the low cost, easy synthesis, and non-toxicity of carbon quantum dots provide significant advantages in terms of practical application, their use as catalyst support material in hydrogen fuel technology is expected to increase rapidly. [15-18].

The major qualities sought after in a support material for catalysts are inertness, porosity, stable components, and the ability to allow surface width [19]. One of the structures utilized as a support material in catalytic processes is activated carbon, which has the listed qualities.

In the context of this investigation, while the pore structure of the hydrothermally produced activated carbon expands more, this circumstance also permits the catalyst's active surface to expand more. The various metal loading to activated carbon ratios helps to clarify this case.

2. Method

The waste product (MDF powder) used in the production of activated carbon was obtained from the furniture industry. First, the hydrothermal process was used to produce the hidrochar. Hidrochar was generated by hydrothermally preserving MDF powder in an autoclave with distilled water for six hours at 180 °C. Then, to produce activated carbon, different activator ratios, activation times, and baking temperatures were altered with the aid of a sodium hydroxide (NaOH) activator. The best activation conditions were determined according to the iodine number determination (ASTM D 4607 standard). By adding various amounts of cobalt metal to activated carbon after it has been created, catalyst manufacturing is made possible [20].

The support material and catalyst have been integrated using the impregnation technique [21]. For this, distilled water was stirred with the specified amounts of metal and activated carbon at 750 rpm for 24 hours. Then, the reduction of the catalyst was achieved by the reduction process under $NaBH_4$ at the determined ratios. Following the necessary cleaning and filtration steps, the catalyst was dried in an oven at 70 °C for 8 hours so that it could be used in the hydrolysis procedure.

The factors affecting catalyst efficiency (solution medium, amount of catalyst, concentration of hydrogen source, and temperature) were identified once the optimum metal ratio was established. The amount of hydrogen produced by hydrolysis was used to calculate the catalyst's efficiency. Figure 1 shows the experimental setup used to calculate the hydrogen ratio.

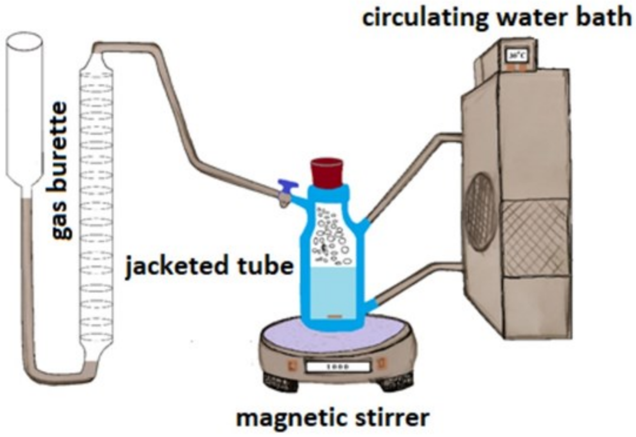

Figure 1. Hydrolysis reaction setup.

A rotating water bath that regulates temperature, a magnetic stirrer, a jacketed tube, a graduated burette, and hoses make up the hydrolysis experiment setup. The jacketed tube offers the experimental setting, while the magnetic stirrer gives the reaction at the standard value. The amount of hydrogen gas released over time is measured with the help of a graduated burette.

3. Results and discussion

3.1. Activated carbon production parameters

The ideal parameters for the production of activated carbon (activator ratio, activation time, baking time, and temperature) were examined [22]. NaOH at concentrations of 20%, 50%, 70%, and 100% was used in experiments to determine the optimum activator ratio while the sample was kept a room temperature for 24 hours. After the activation (impragment) process, activated carbon was produced at 500 ⁰C with a 45 min baking time. The resulting activated carbon's iodine number was measured after washing and drying. Figure 2(a) shows the results of the iodine number of activated carbon. Accordingly, the best activator ratio was determined as 70% NaOH. The activation time parameter was investigated for 12, 24, 36, and 48 hours in room conditions, and it was found that 24 hours was the ideal activation period (Figure 2(b)). The samples were baked for several amounts of time (30, 45, 60, and 90 minutes) in the gas oven to assess the influence of baking time (Figure 2(c)).

According to Figure 2(c), the ideal baking time was determined as 45 minutes. The impact of temperature was then investigated. For this, the samples were kept at various temperatures (400, 500, 600, and 700 ⁰C) in an oven (Figure 2d). Figure 2(d) shows that the iodine number rises as a result of the rising temperature. As a result, it was determined that 700 ⁰C was the ideal temperature.

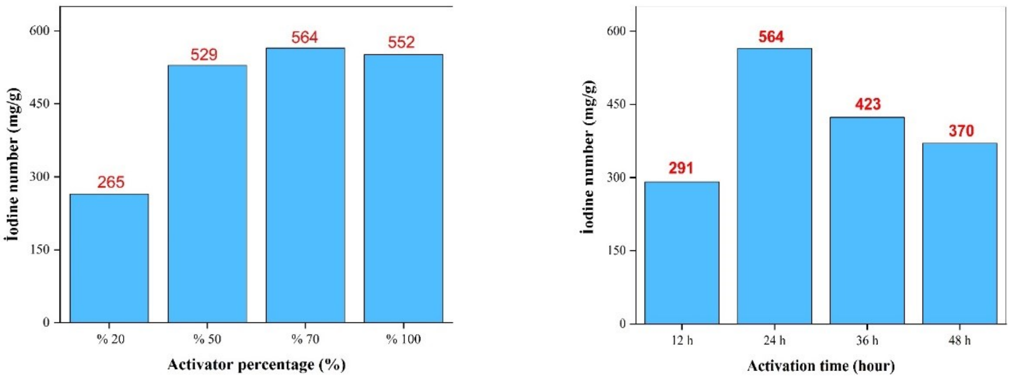

a) Activator (NaOH) percentage

b) Activation time

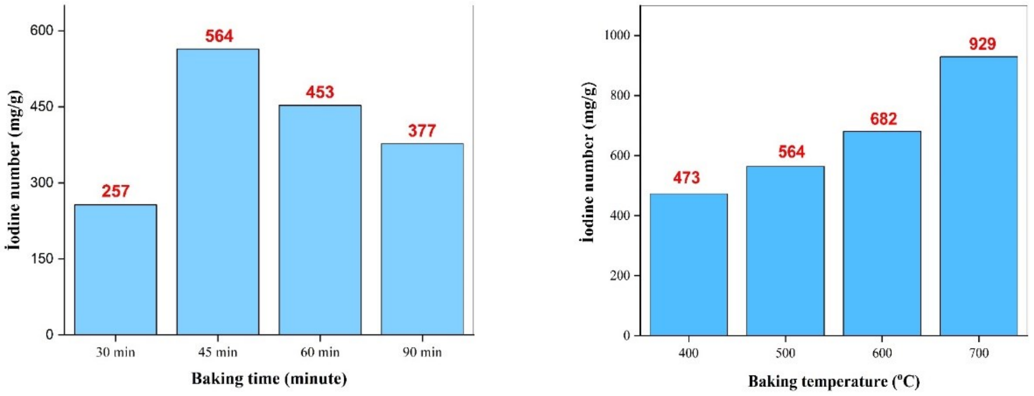

c) Baking time

d) Baking temperature

Figure 2. Activated carbon production conditions.

3.2. Characterization of activated carbon

After determining the optimum conditions, the structural analysis of the activated carbon produced under these conditions was examined. TG/DTA, EDX, and SEM analyses were carried out. Figure 3 shows the TG/DTA analysis of MDF powder utilized as an activated carbon source. Accordingly, at 472 ºC, 99.9% of the MDF powder by mass was removed from the atmosphere.

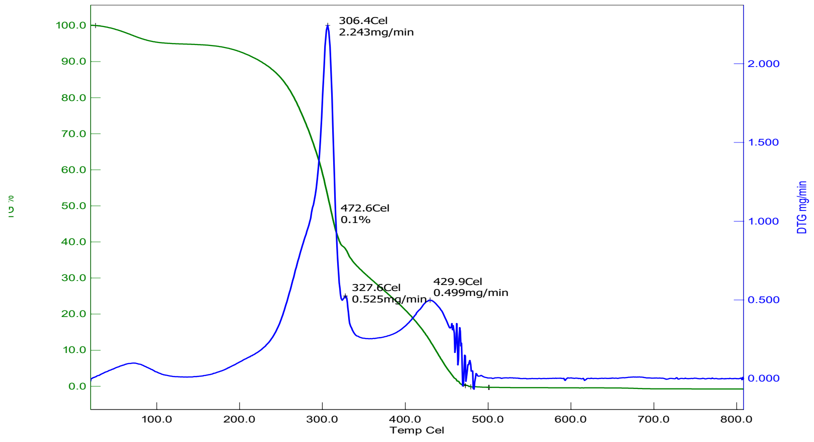

Figure 3. TG/DTA analysis of MDF powder.

The TG/DTA analysis of hydrochar obtained after hydrothermal pretreatment is given in Figure 4(a). It is clear from Figure 4(a) that the decomposition temperature of the entire hydrochar is higher even though the temperature-dependent decomposition values of hydrochar exhibit similar properties to MDF powder. Figure 4(b) shows the results of the TG/DTA analysis of the generated activated carbon. Figure 4(b) shows that the amount of temperature-related decomposition in MDF powder and hydrochar is expressed in mg, but the value for activated carbon is expressed in g. This shows that the structure of activated carbon is resistant to temperature. The decomposition accelerates above 700 °C, the temperature at which activated carbon is produced. Reference researches also highlight similar degradation curves [23,24].

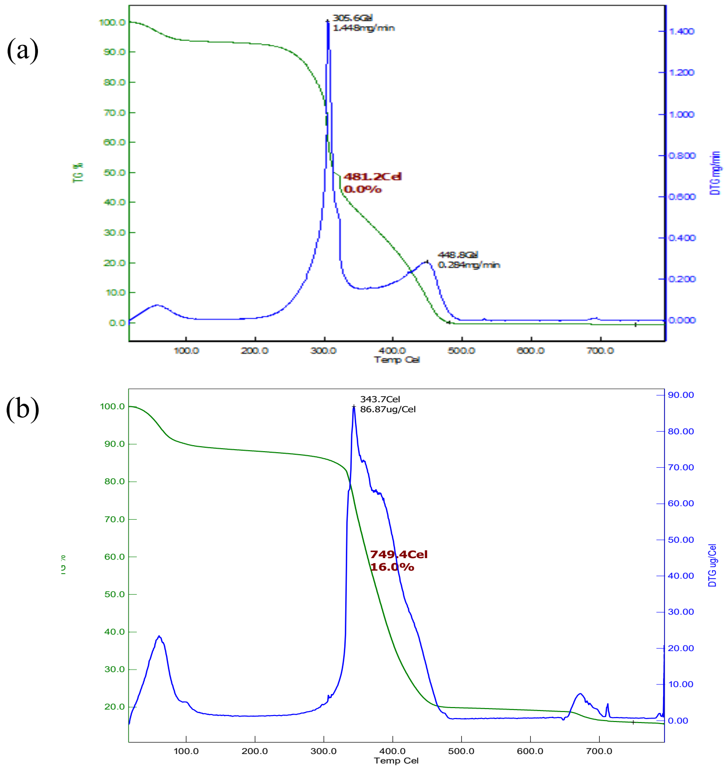

Figure 4. TG/DTA analysis of a) hydrochar b) activated carbon.

Figure 5 displays the outcomes of the EDX analysis carried out to ascertain the element ratio in the structure of activated carbon. According to Figure 5, the carbon element makes up the majority of active carbon (70%). Additionally, NaOH, which is used as an activator, is successfully attached to the surface of the activated carbon. Calcium in the structure of activated carbon is the heteroatom in the organic structure [25].

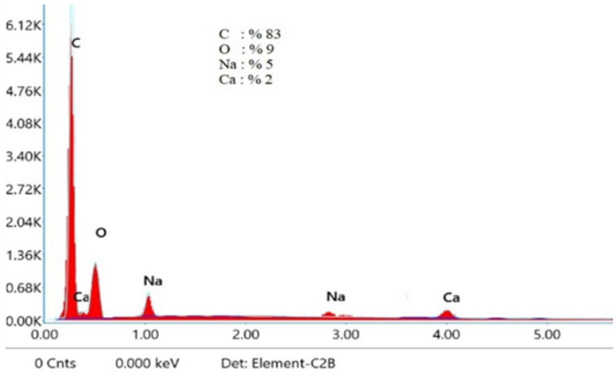

Figure 5. EDX analysis of activated carbon.

Figure 6 shows SEM images of activated carbon in sizes of 1 and 10 µm. Activated carbon has a large porous surface structure.

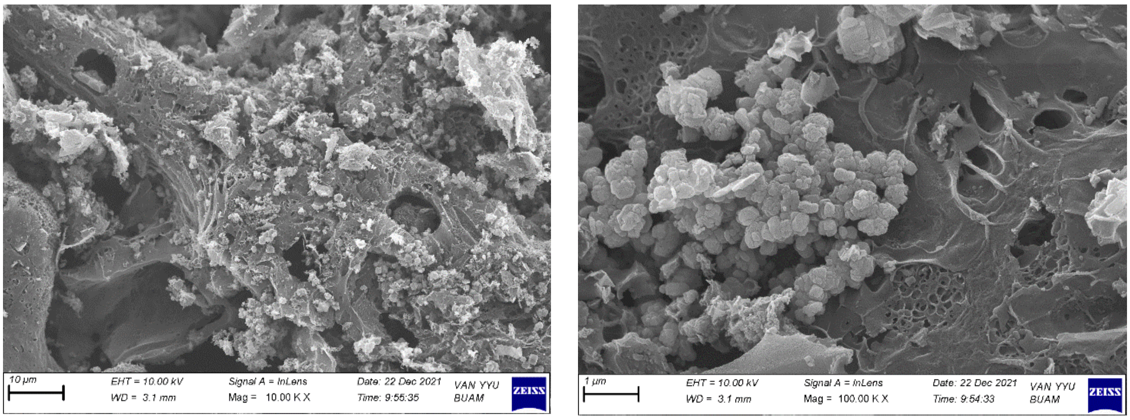

Figure 6. SEM images of activated carbon.

3.3. Synthesis of catalyst and examination of hydrolysis data

3.3.1. Determining the metal ratio for the catalyst

Cobalt (Co) metal was selected as the metal for catalyst manufacture because of its low cost and great efficiency. First, the sodium borohydride ($NaBH_4$) hydrolysis tested in the presence of a pure cobalt catalyst resulted in a hydrogen generation rate of 3872.8 ml/g.min. at 303 K.

Metal ratios of 10%, 20%, 30%, and 40% were investigated to study the impact of metal content on catalyst effectiveness by using 5 and 50 mg catalysts. The influence of the metal ratio on hydrogen production by hydrolysis reaction (in the presence of 5% NaOH at 30 ^{0}C) is depicted in Figures 7 (with 5 mg catalyst) and 9 (with 50 mg catalyst). Figures 7 and 8 show that using 70% activated carbon and 30% cobalt led to the best hydrogen production rate.

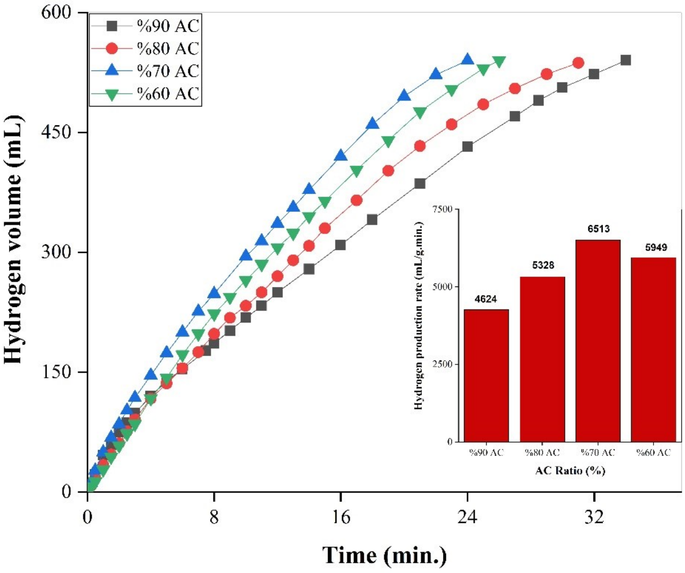

Figure 7. Effect of different metal ratios on hydrogen production (with 5 mg catalyst).

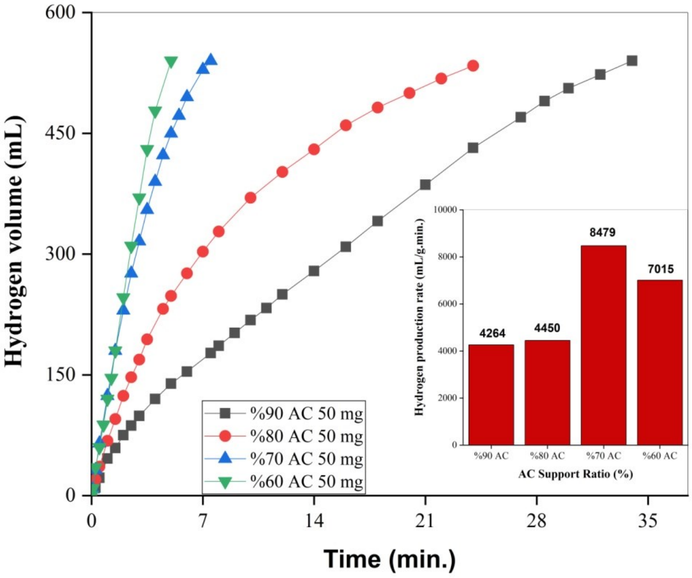

Figure 8. Effect of different metal ratios on hydrogen production (with 50 mg catalyst).

3.3.2. Characterization of Co@AC catalyst

The catalyst's FT-IR spectrum is displayed in Figure 9. The weak band at 630 cm^{-1} is hypothesized to be caused by a putative Co and oxygen interaction [26]. The C=C and C=O vibrations are responsible for the peaks at around 2000-2100 cm^{-1} [27].

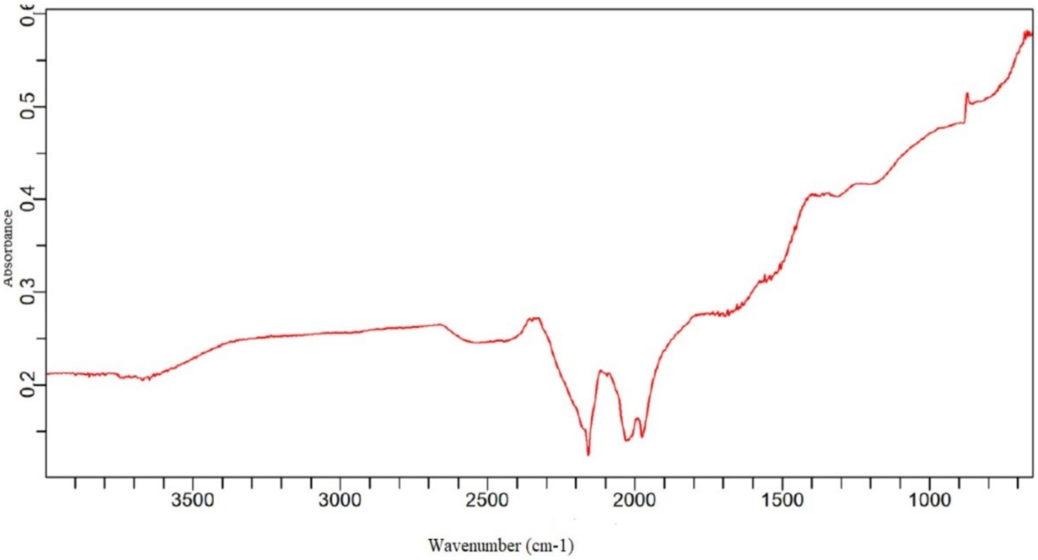

Figure 9. FT-IR spectrum of catalyst (70% Activated carbon 30% Cobalt).

Figure 10 presents the results of the catalyst's EDX examination. The results of the EDX analysis show that the activated carbon-supported cobalt catalyst has been synthesized successfully.

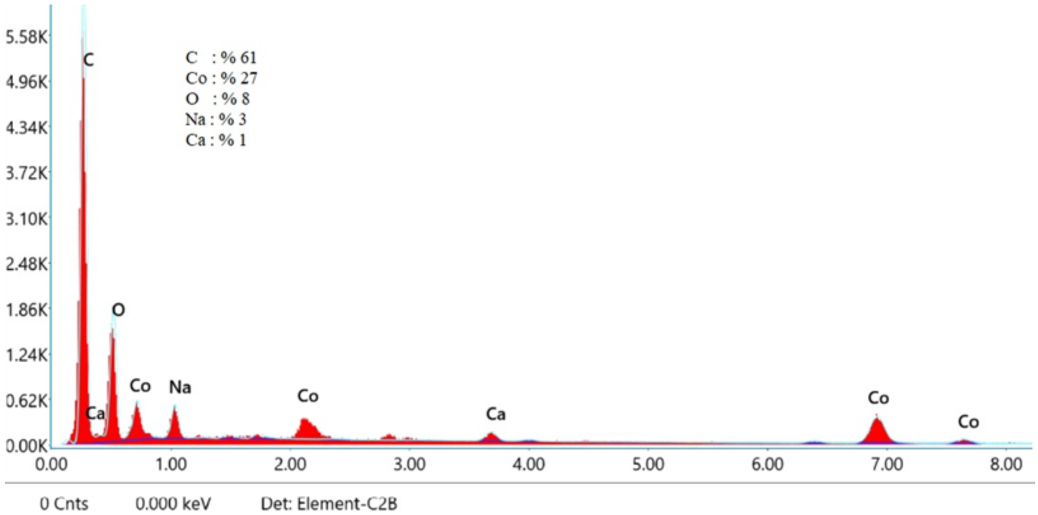

Figure 10. EDX analysis of catalyst.

Figure 11 shows SEM images of pure cobalt catalysts and cobalt catalysts supported by activated carbon. The SEM images show that the pure cobalt catalyst is clumped together, but this clumping is not present in the cobalt catalyst supported by activated carbon. As a result, the catalyst's active surface was enhanced by the activated carbon support, increasing the rate of hydrogen production.

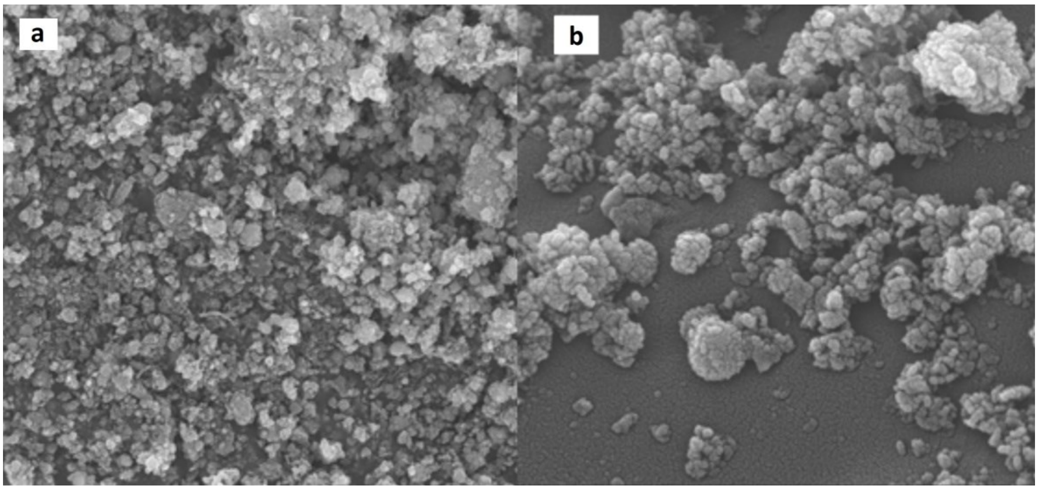

Figure 11. SEM images of a) pure cobalt b) activated carbon@cobalt catalyst.

3.3.3. Effect of solution ratio

In addition to acting as the hydrogen source, sodium borohydride (NaOH) was used as the solvent. Figure 12 provides a graph illustrating how the concentration of NaOH affects hydrolysis. As a result of hydrolysis experiments performed to prevent sodium borohydride from spontaneously hydrolyzing, even slightly, and to ascertain the solvent effect on the catalyst activity, it was found that a sodium hydroxide ratio of 5% produced the best hydrogen production rate per gram of catalyst.

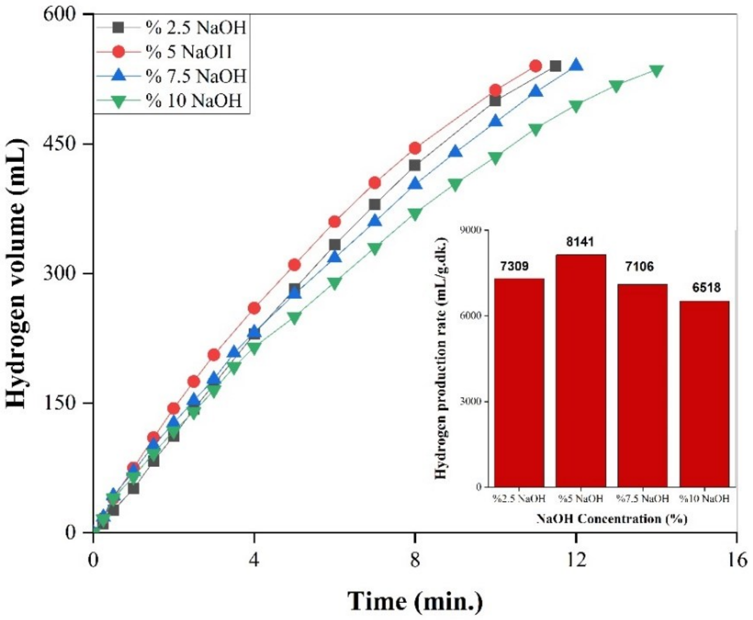

Figure 12. The effect of solution ratio on hydrogen production.

3.3.4. The effect of catalyst amount

Different catalyst amounts were used in hydrolysis processes to test the impact of catalyst amount on the rate of hydrogen production (Figure 13). Figure 13 illustrates how the amount of catalyst used causes the hydrolysis reactions to complete more quickly. Additionally, the catalyst dose of 40 mg produced the most hydrogen at the best rate. This is due to the optimal value being provided by the substrate density that corresponds to the catalyst surface [28].

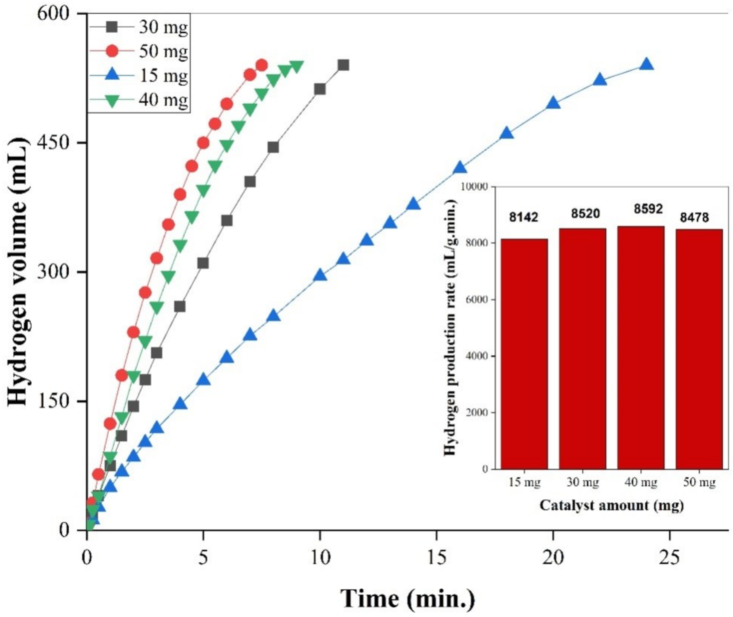

Figure 13. Effect of catalyst amount on hydrogen production.

3.3.5. The effect of the concentration of $NaBH_4$

Using $NaBH_4$ at ratios of 1%, 2%, 3%, and 4%, experiments were conducted to ascertain the impact of $NaBH_4$ concentration on hydrogen production (Figure 14). According to Figure 14, a slight decrease in the rate of hydrogen production was observed with the increase in the amount of $NaBH_4$. Because, the catalytic activity is inhibited as a result of sodium metaborate, which is a product of the hydrolysis reaction [29]. The best hydrogen production rate depending on the concentration change was obtained with the use of 2% $NaBH_4$ [30,31].

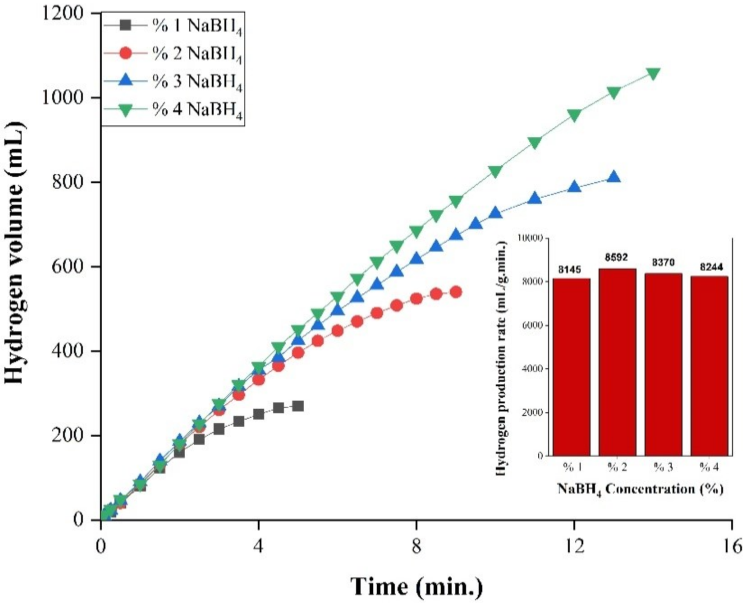

Figure 14. Effect of $NaBH_4$ concentration on hydrogen production.

3.3.6. The effect of the temperature

Temperature is a key factor being researched in the creation of hydrogen. The measurement of the temperature effect serves two basic objectives. To possibly use it, the catalyst's effect is first observed at various temperatures, and then the reaction kinetics are established. To examine the temperature effect, the hydrolysis reaction was studied at 30 and 60 ^{0}C temperatures. Figure 15 shows this effect. Figure 15 shows that the rate of hydrogen production increased with temperature. While the hydrogen production rate was 8592 ml/g.min at 30 ^{0}C, it increased to 38012 ml/g.min at 60 ^{0}C.

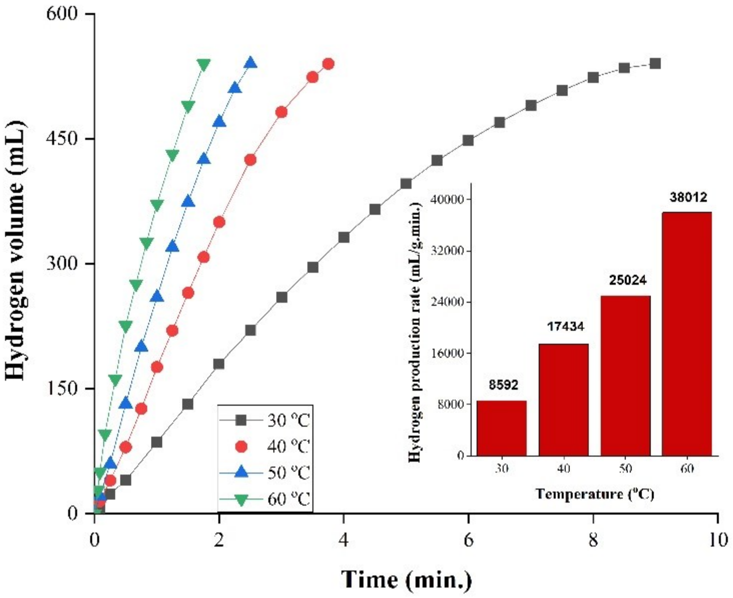

Figure 15. The effect of temperature on hydrogen production.

3.4. Reaction kinetics and repeated use of catalyst

The results of the studies at various temperatures showed that the hydrolysis reaction follows the n. order reaction kinetics. The catalysis reaction of $NaBH_4$ hydrolysis can be described by the Arrhenius equation given in Equation 3.

$$lnk = lnA\text{-}Ea / RT \qquad (3)$$

Here;
k is the rate constant (min-1), A is an Arrhenius factor, R is the universal gas constant (8.314 kJ K^{-1} mol^{-1}), and T is the absolute temperature (K). The data from the hydrolysis reaction carried out at various temperatures were used to plot the 1/T graph against lnk and produce Figure 16. The activation energy (Ea) of the reaction is determined to be 31.19 kJ mol^{-1} by substituting the slope value of the curve in Figure 16 into the Arrhenius equation [32,33].

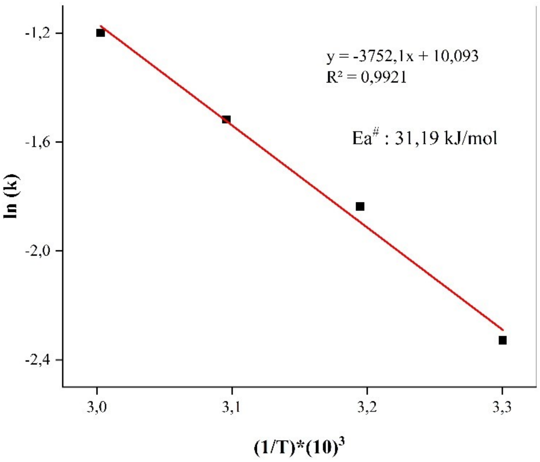

Figure 16. The plot of 1/T vs. ln k.

Table 1 provides information on the catalytic process and temperature-dependent values of hydrogen production under ideal circumstances.

Table 1. Hydrolysis reaction data

Temperature (°C)	**Hydrogen production rate (ml/g min)**	**Reaction degree**	**R^2**	**k**
30	8592.5	n. degree	0.9998	0.0974
40	17434.17	n. degree	0.9983	0.1594
50	25024.17	n. degree	0.9992	0.2193
60	38012.5	n. degree	0.9982	0.3016

The liquid that remained on the top of the catalyst after each usage was allowed to collapse was permitted to be removed from the environment by decantation, ensuring that the catalyst could be used repeatedly. By incorporating the amount of solution taken from the environment, the hydrolysis of the Co@AC catalyst product up until the sixth use was examined [34]. It has been determined that it provides 100% efficiency until the end of the 6th use (Figure 17).

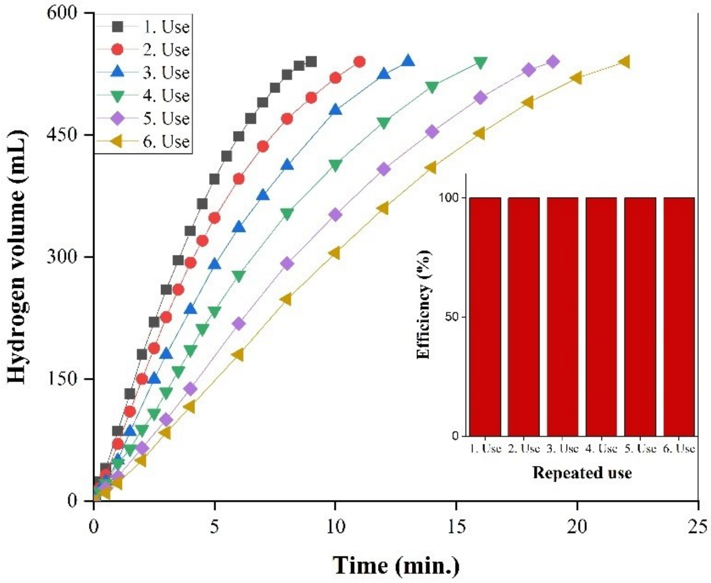

Figure 17. Hydrogen production by repeated use of the catalyst.

4. Conclusion

Activated carbon was produced in this study to provide support material for the cobalt catalyst in the hydrolysis reaction of $NaBH_4$. Catalyst synthesis was performed at different metal and active carbon ratios, and the best combination value was determined as 70% activated carbon and 30% metal. Concerning the sodium borohydride hydrolysis data, the effectiveness of the produced catalysts was evaluated. When a catalyst containing 70% active carbon was used in the hydrolysis reaction instead of a catalyst composed wholly of cobalt, the production rate of hydrogen rose from 3872.8 to 6513.6 ml/g min. As a result of the optimization studies of the catalyst, it was determined that the best hydrogen production rate was at 30 °C, using 5% NaOH, 40 mg catalyst, and 2% $NaBH_4$ by mass. The hydrogen production rate under these conditions was determined as 8592.5 ml/g min. The kinetic route of the hydrolysis reaction was found to be of the n. order, with an activation energy of 31.19 kJ/mol. The increased rate of hydrogen production indicates that using activated carbon as a support material greatly enhances the cobalt catalyst's capacity to perform its function.

References

[1] Arsad, A. Z., Hannan, M. A., Al-Shetwi, A. Q., Mansur, M., Muttaqi, K. M., Dong, Z. Y. and Blaabjerg, F., Hydrogen energy storage integrated hybrid renewable energy systems: A review analysis for future research directions, ***International*** **Journal of Hydrogen Energy**, 47, 17285-17312, (2020).

[2] İzgi, M. S., Ece, M. Ş., Kazici, H. Ç., Şahin, Ö. and Onat, E., Hydrogen production by using Ru nanoparticle decorated with Fe_3O_4@ SiO_2–NH_2 core-shell microspheres, **International Journal of Hydrogen Energy**, 45, 55, 30415-30430, (2020).

[3] İzgi, M. S., Şahin, Ö., Onat, E. and Saka, C., Epoxy-activated acrylic particulate polymer-supported Co–Fe–Ru–B catalyst to produce H_2 from hydrolysis of NH_3BH_3, **International Journal of Hydrogen Energy**, 45, 43, 22638-22648, (2020).

[4] Boretti, A., Production of hydrogen for export from wind and solar energy, natural gas, and coal in Australia, **International Journal of Hydrogen Energy,** 45, 7, 3899-3904, (2020).

[5] Kim, K. C. & Sholl, D. S., Crystal structures and thermodynamic investigations of LiK $(BH_4)_2$, KBH_4, and $NaBH_4$ from first-principles calculations, **The Journal of Physical Chemistry C**, 114, 1, 678-686, (2010).

[6] Dincer, İ., Technical, environmental and energetic aspects of hydrogen energy systems, **International Journal of Hydrogen Energy**, 27, 3, 265-285, (2002).

[7] Onat, E., Aslan, M. and İzgi, M. S., Kobalt bazli bimetalik nanokatalizörün potasyum borhidrür hidroliz tepkimesi üzerindeki katalitik etkisinin incelenmesi, **Konya Mühendislik Bilimleri Dergisi**, 9, 200-212, (2021).

[8] Jain, I. P., Jain, P. and Jain, A., Novel hydrogen storage materials: A review of lightweight complex hydrides, **Journal of Alloys and Compounds**, 503, 2, 303-339, (2010).

[9] Şahin, Ö., İzgi, M. S., Onat, E. and Saka, C., Influence of the using of methanol instead of water in the preparation of Co–B–TiO_2 catalyst for hydrogen production by $NaBH_4$ hydrolysis and plasma treatment effect on the Co–B–TiO_2 catalyst, **International Journal of Hydrogen Energy**, 41, 4, 2539-2546, (2016).

[10] Muir, S. S. & Yao, X., Progress in sodium borohydride as a hydrogen storage material: Development of hydrolysis catalysts and reaction systems, **International Journal of Hydrogen Energy,** 36, 10, 5983-5997, (2011).

[11] Török, B., Schäfer, C. and Kokel, A., **Heterogeneous Catalysis in Sustainable Synthesis**, eBook ISBN: 9780128178263, 23-80, (2022).

[12] Armarego, W. L. F., Purification of Laboratory Chemicals (Ninth edition), Butterworth-Heinemann, eBook ISBN: 978-0-323-90968-6, 241-363, (2022).

[13] Taştaban, M., Katalitik ıslak peroksit oksidasyonu yoluyla azo boyar madde gideriminde kullanılmak üzere bentonit destekli katalizör sentezi ve karakterizasyonu, Doktora Tezi, Osmangazi Üniversitesi, Fen Bilimleri Enstitüsü, Eskişehir, (2019).

[14] Mehrabadi, B. A. T., Eskandari, S., Khan, U., White, R. D. and Regalbuto, J. R., A Review of Preparation Methods for Supported Metal Catalysts, **Advances in Catalysis**, 61, 1-35, (2017).

[15] Onat, E., Horoz, S., Şahin, Ö. and İzgi, M. S., Revolutionary carbon quantum dot supported-Co catalyst for record-breaking hydrogen production rate, **Journal of the Australian Ceramic Society,** 1-10, (2024).

[16] Onat, E., Izgi, M. S., Şahin, Ö. and Saka, C., Highly active hydrogen production from hydrolysis of potassium borohydride by caffeine carbon quantum dot-supported cobalt catalyst in ethanol solvent by hydrothermal treatment, **International Journal of Hydrogen Energy,** 51, 362-375, (2024).

[17] İzgi, M. S., Onat, E., Şahin, Ö. and Saka, C., Green and active hydrogen production from hydrolysis of ammonia borane by using caffeine carbon quantum dot-supported ruthenium catalyst in methanol solvent by hydrothermal treatment, **International Journal of Hydrogen Energy**, 51, 180-192, (2024).

[18] Onat, E., İzgi, M. S., Şahin, Ö. and Saka, C., Nickel/nickel oxide nanocomposite particles dispersed on carbon quantum dot from caffeine for hydrogen release by sodium borohydride hydrolysis: Performance and mechanism, **Diamond and Related Materials,** 141, 110704, (2024).

[19] Hagen, J., **Industrial catalysis: a practical approach**, John Wiley & Sons, eBook ISBN: 978-3-527-33165-9, (2015).

[20] Yaslı, M.A., Antep fıstığı kavlatma tesisi atıklarından hidrotermal yöntemle aktif karbon üretimi, Yüksek Lisans Tezi, Fırat Üniversitesi, Fen Bilimleri Enstitüsü, Elazığ, (2005).

[21] White, R.J., Luque, R., Budarin, V. L., Clark, J. H., Macquarrie, D. J., Supported metal nanoparticles on porous materials. Methods and applications, **Chemical Society Reviews**, 38, 2, 481-494, (2009).

[22] Mahanim, S. M. A., Asma, I. W., Rafidah, J., Puad, E. and Shaharuddin, H., Production of activated carbon from industrial bamboo wastes, **Journal of Tropical Forest Science**, 417-424, (2011).

[23] Le Van, K. and Thi, T. T. L., Activated carbon derived from rice husk by NaOH activation and its application in supercapacitor, **Progress in Natural Science: Materials International**, 24, 3, 191-198, (2014).

[24] Oliveira, A. V., Vilaça, R., Santos, C. N., Costa, V. and Menezes, R., Exploring the power of yeast to model aging and age-related neurodegenerative disorders, **Biogerontology,** 18, 1, 3-34, (2017).

[25] Shin, D. Y., Sung, K. W. and Ahn, H. J., Synergistic effect of heteroatom-doped activated carbon for ultrafast charge storage kinetics, **Applied Surface Science**, 478, 499-504, (2019).

[26] Nakamoto, K., **Infrared spectra of Inorganic and Coordination Compounds**, 2nd ed. New York, John Wiley and Sons, (1963).

[27] Liu, Y., Liu, X., Dong, W., Zhang, L., Kong, Q. and Wang, W., Efficient Adsorption of Sulfamethazine onto Modified Activated Carbon: A Plausible Adsorption Mechanism, **Scientific Reports**,7, 12437, (2017).

[28] Onat, E., Şahin, Ö., Izgi, M. S. and Horoz, S., An efficient synergistic Co@ CQDs catalyst for hydrogen production from the hydrolysis of NH_3BH_3, **Journal of Materials Science: Materials in Electronics**, 32, 27251-27259, (2021).

[29] İzgi, M. S., Effect of microwave irritated Co-B-Cr catalyst on the hydrolysis of sodium borohydride, **Energy Sources, Part A: Recovery, Utilization, and Environmental Effects**, 38, 17, 2590-2597, (2016).

[30] Li, Z., Li, H., Wang, L., Liu, T., Zhang, T., Wang, G. and Xie, G., Hydrogen generation from catalytic hydrolysis of sodium borohydride solution using supported amorphous alloy catalysts (Ni–Co–P/γ-Al_2O_3), **İnternational journal of hydrogen energy,** 39, 27, 14935-14941, (2014).

[31] Demirci, U. B., Akdim, O., Hannauer, J., Chamoun, R. and Miele, P., Cobalt, a reactive metal in releasing hydrogen from sodium borohydride by hydrolysis: A short review and a research perspective, **Science China Chemistry,** 53, 1870-1879, (2010).

[32] Onat, E., & Ekinci, S., A new material fabricated by the combination of natural mineral perlite and graphene oxide: Synthesis, characterization, and methylene blue removal, **Diamond and Related Materials,** 110848, (2024).

[33] İzgi, M. S., Şahin, Ö., Onat, E. and Horoz, S., Metanolde sentezlenen Co-B katalizörün sodyum hidrolizi üzerine etkisi, **Journal of the Institute of Science and Technology,** 7, 4, 151-160, (2017).

[34] Lee, J., Shin, H., Choi, K. S., Lee, J., Choi, J. Y. and Yu, H. K., Carbon layer supported nickel catalyst for sodium borohydride ($NaBH_4$) dehydrogenation, **International Journal of Hydrogen Energy,** 44, 5, 2943-2950, (2019).